Results in Physics 7 (2017) 3624–3633

Contents lists available at ScienceDirect

Results in Physics

journal homepage: www.journals.elsevier.com/results-in-physics

Polyacrylamide ferrogels with embedded maghemite nanoparticles for biomedical engineering

Felix A. Blyakhman [a,b,*], Alexander P. Safronov [b,c], Andrey Yu. Zubarev [b], Tatyana F. Shklyar [a,b], Oleg G. Makeyev [a], Emilia B. Makarova [a,d], Vsevolod V. Melekhin [a], Aitor Larrañaga [e], Galina V. Kurlyandskaya [b,e]

[a] Ural State Medical University, 620028 Yekaterinburg, Russia
[b] Ural Federal University, 620002 Yekaterinburg, Russia
[c] Institute of Electrophysics, RAS, Urals Branch, 620016 Yekaterinburg, Russia
[d] Ural Institute of Traumatology and Orthopedics, 620000 Yekaterinburg, Russia
[e] University of the Basque Country UPV-EHU, 48940 Leioa, Spain

ARTICLE INFO

Article history:
Received 23 June 2017
Received in revised form 11 September 2017
Accepted 19 September 2017
Available online 23 September 2017

Keywords:
Hydrogel
Magnetic nanoparticles
Viscoelasticity
Electrical potential
Cells adhesion
Biomedical engineering

ABSTRACT

This study addresses the development of gel-based magnetic material in the purposes of biomedical applications in the fields of tissue engineering, regenerative medicine, drugs delivery and magnetic biosensing. Ferrogels were synthesized by radical polymerization of acrylamide in a stable aqueous suspension of γ-$Fe_{2.04}O_{2.96}$ nanoparticles (NPs) fabricated by the laser target evaporation technique. Gel network density was set to 1:100, the concentrations of imbedded NPs (average mean diameter of about 11 nm) were fixed at 0.00, 0.25 or 0.75% by weight. Saturation magnetization of the gels showed a linear dependence on concentration of NPs. The main task of proposed investigation was to determine the contribution of the presence of NPs to the change of the physical properties of gels and their biocompatibility. We found that the gradual increase of NPs concentration in the gel network resulted in the significant increase of the gel's Young modulus, effective viscosity, negative value of electrical potential and adhesion index for both the human dermal fibroblasts and the human peripheral blood leucocytes. We concluded that from viewpoint of biomedical applications, the inclusion of small amount of NPs into the polymer network significantly enhances the mechanical and electrical properties of ferrogels, and improves biocompatibility of these systems.

Introduction

Recently, magnetic nanoscale particles had received significant interest due to their intrinsic properties in the expectation of the biomedical applications employing their ability to respond on the application of the magnetic field. Magnetic materials can be used for magnetic separation, magnetic biosensing, *in vivo* medical imaging, drug delivery, thermal ablation or hyperthermia and tissue repair [1]. Iron oxide nanoparticles (NPs) without surface modification usually display hydrophobic properties causing their agglomeration, plasma opsonin protein adsorption, recognition by the microphages and removal from the blood stream within seconds [2]. The way to avoid these obstacles is to design water-based stabilized (sterically or electrostatically) magnetic suspensions with requested properties. That is, magnetic ferrofluids become the next generation magnetic materials for biomedical applications. Further development of the concept of biomedical magnetic nanomaterials resulted in appearance of polymer/NPs composites, such as magnetic microspheres for magnetic separation or magnetic label detection [3] and finally ferrogels [4].

In general, gel is a 3D cross-linked polymer network swollen in a liquid phase [5,6]. The physical basis of functional properties of the polyelectrolyte hydrogels stems from the balance of interaction of polymeric filaments with the medium, the entropic flexibility of filaments, the positive osmotic pressure of counterions, and the balance of forces of attraction and repulsion between electric charges [7].

The structure of gel-like synthetic systems is similar to the living systems where the biopolymer network is immersed into a liquid phase. Typical example of the gel-like biological system is the cell cytoskeleton. Remarkably, the synthetic gels mimic well a number of cell functions, e.g. contraction, elongation,

* Corresponding author at: Ural State Medical University, 620028 Yekaterinburg, Russia.
E-mail address: Feliks.Blyakhman@urfu.ru (F.A. Blyakhman).

https://doi.org/10.1016/j.rinp.2017.09.042
2211-3797/

electrocapacity, secretion etc. [8–11]. Close resemblance of the structural and functional features of gel-like synthetic and living systems is the most important argument for implication of synthetic hydrogels in biomedical applications.

The development of biocompatible materials based on the functional properties of gels is a promising area of biomedical engineering. In particular, polyacrylamide (PAAm) gels and their copolymers are widely introduced as a soft working body of sensors, actuators and transducers [12,13]. Furthermore, the advantages of PAAm gels as the cellular substrates for tissue engineering were reported in a number of investigations [14–17].

Meanwhile, resent studies have demonstrated a new class of hydrogels filled with the magnetic nanoparticles [18–20]. On the one hand, the iron oxide NPs *per se* have many application in medicine, e.g. for MRI diagnostics, drugs targeted delivery and controlled release, hyperthermia treatment of tumors, magnetic biosensing and so on [1,21,22]. On the other hand, the composition of hydrogel and iron oxide NPs opens up a potential in the development of magnetically controlled biocompatible materials for tissue engineering, regenerative medicine, drugs delivery and magnetic biosensing [22–26].

In our early works, the electromechanical [27,28] and mechano-electrical transductions [29,30] in copolymers of PAAm gels were studied in details. Taking into account the future development of ferrogels in biomedical applications, this study was aimed to determine the impact of iron oxide NPs on the gel functional properties. In this work, we discuss our experience of PAAm-based ferrogels fabrication and characterization and the influence of NPs concentration on the gel's Young modulus, effective viscosity, electrical potential and degree of the cell adhesion. We show that from the viewpoint of biomedical applications, the inclusion of small amount of iron oxide NPs (0.25 or 0.75 wt%) into the polymer network of PAAm gel significantly enhances the mechanical and electrical properties of ferrogels, and improves the biocompatibility of these systems.

Materials and methods

Materials

Magnetic nanoparticles for the synthesis of ferrogels

Iron oxide NPs were synthesized by laser target evaporation (LTE) of Fe_2O_3 target pellet using specialized setup with Yb fiber laser operated in pulse regime at 1.07 μm wavelength [31]. This very productive method of high-energy physical dispersion was extensively described in our earlier works [32,33]. Fig. 1 shows transmission electron microscopy (TEM) image of NPs obtained by JEOL JEM2100 microscope: NPs were spherical and non-agglomerated. Particle size distribution (PSD) of MNPs was obtained by the analysis of TEM images in the ensemble of 2160 particles. PSD (Fig. 1 inset) was lognormal with the median value 11.4 nm and dispersion 0.423. 90% of NPs by weight had the diameter below 30 nm.

The specific surface area of NPs (S_{sp}) measured by the low-temperature adsorption of nitrogen (Micromeritics TriStar 3000) was 78.0 m^2/g. The weight average diameter of NPs, calculated from this value using the equation $d_w = 6/(\rho S_{sp})$ ($\rho = 4.6$ g/cm^3 being the density of iron oxide) was 16.7 nm, i.e. in a good agreement with $d_w = 18.5$ nm, obtained using PSD with the parameters given above.

The crystalline structure of NPs was characterized by X-ray diffraction (XRD) using Bruker D8 Discover diffractometer (Fig. 2). The peaks in the diffractogram corresponded to inverse spinel structure, which is basically the same for magnetite and maghemite. The exact chemical composition of MNPs determined by the electrochemical Red-Ox titration (TitroLine, Schott Instruments) was found to be $Fe_{2.04}O_{2.96}$, that is close to maghemite. A detailed discussion on the crystalline and chemical structure of LTE iron oxide NPs was provided in our previous report [34].

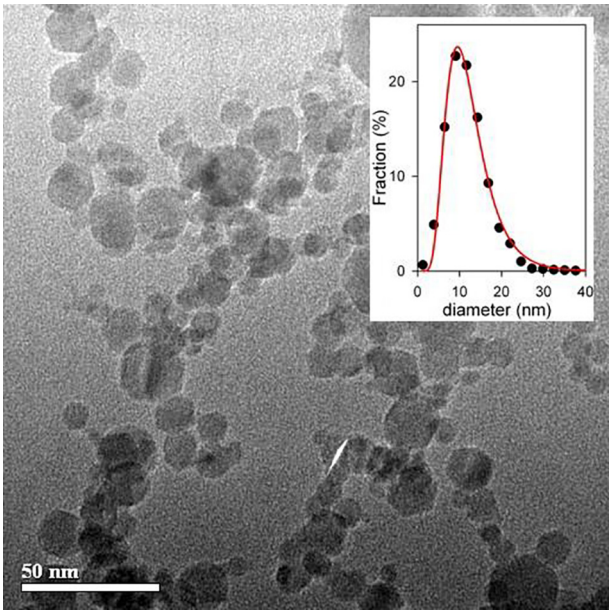

Fig. 1. TEM image of iron oxide NPs (JEOL JEM2100). Inset: PSD of MNPs obtained by graphical analysis of images (2160 particles).

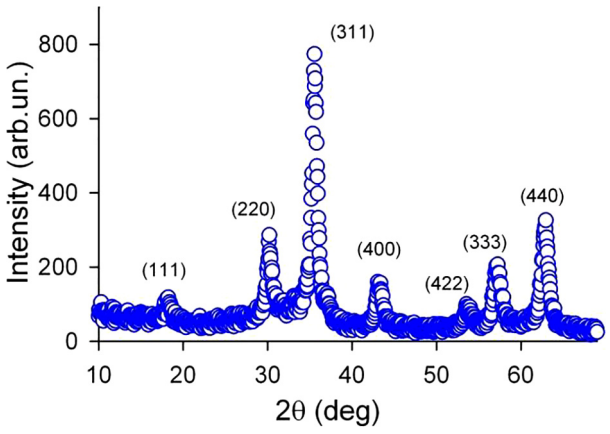

Fig. 2. XRD pattern of iron oxide NPs with corresponding Miller indexes identification.

Hysteresis loops and termomagnetic curves of the iron oxide NPs were measured by MPMS XL-7 SQUID-magnetometer. Fig. 3 shows the hysteresis loop of air-dry NPs measured at room temperature. One can appreciate rather low but not exactly zero coercivity consistent with the average size obtained by structural evaluation.

Observed magnetic behaviour of the studied particles was previously described in terms of core-shell structure of individual nanoparticle taking into account the effect of the interaction of the core magnetization and the shell of the particle [32]. The value of the saturation magnetization (M_s) obtained for spherical LTE NPs was close to 55 emu/g being quite reasonable for the iron oxide NPs of this size. It is necessary to mention that even at 5 K, the magnetization curves did not saturate and the maximum magnetization value in a field of 60 kOe was denoted as M_s. It was appreciably smaller than the one expected for bulk maghemite.

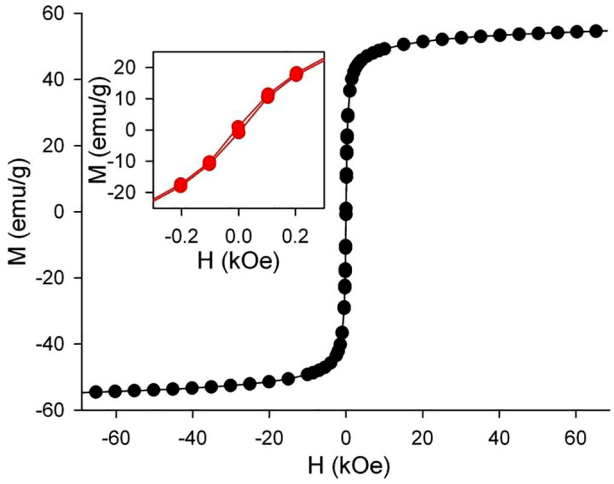

Fig. 3. Hysteresis loop of iron oxide NPs measured at room temperature. Inset: magnified part of the M(H) loop in low fields.

This was understood by taking into account the small size of the NPs and the high amount of atoms on the surface.

Indeed, because of defects of the crystalline structure and non-compensated spins, very often the surface layers of ferromagnetic particles are less magnetized than their bulk cores. Obviously, this factor reduces the saturated magnetization of the system of NPs as compared with the bulk magnetic material.

Preparation and characterization of ferrofluid

Based on LTE maghemite NPs the stable ferrofluids were prepared for the synthesis of ferrogels. Air-dry MNPs were dispersed in 5 mM solution of sodium citrate to get 6% (wt) stock suspension. The suspension was ultrasonically treated for 30 min using Cole-Palmer CPX750 processor operated at 200 W output. The decrease in the average hydrodynamic diameter of aggregates in the stock suspension was monitored by dynamic light scattering (DLS) using Brookhaven ZetaPlus analyzer. As the average hydrodynamic diameter decreased to ca. 100 nm, the stock suspension was centrifuged at 9000 rpm for 5 min using Hermle Z383 centrifuge. The supernatant ferrofluid contained 5.04% (wt) of the iron oxide NPs. The average hydrodynamic diameter of particles in ferrofluid was 49.5 ± 0.1 nm. Fig. 4 presents the weighted PSD of particles in ferrofluid by DLS in comparison to the weighted PSD of air-dry NPs by TEM. The major fraction of particles in ferrofluid corresponds to

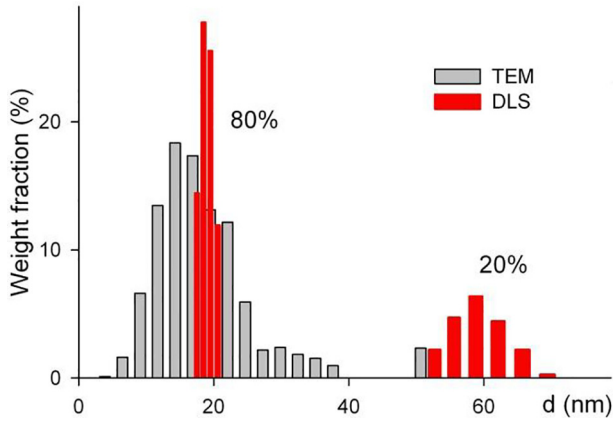

Fig. 4. Histograms of weighted PSD of iron oxide NPs in air-dry state (TEM) and in stabilized water suspension (DLS). Numbers give the weight percentage of fractions in water suspension.

the individual NPs (80% by weight) whereas the minor fraction of small aggregates is still present (20% by weight).

Despite the fact that the major part of the iron oxide NPs by weight had the diameter below 30 nm, a significant amount of NPs (about 10%) corresponds to a larger particles. Their magnetic state is not necessarily corresponds to a material with uniformly magnetized core and even not necessarily corresponds to a single domain state which is close to 30–40 nm for maghemite [35]. This may explain not exactly zero coercivity of NPs and as it will be discussed below, some peculiarities in agglomeration of MNPs during ferrogel synthesis.

Zeta-potential of ferrofluid was measured by the electrophoretic light scattering (ELS) using Brookhaven ZetaPlus analyzer. It was −30.1 ± 0.7 mV, which value stands for the high stability of the ferrofluid due to the adsorption of electrostatic stabilizer (citrate anions) upon the surface of iron oxide NPs.

Synthesis of gels and ferrogels

Polyacrylamide gels (PAAm) were synthesized by the free-radical polymerization in 1.6 M aqueous solution with N,N′-methy lene-diacrylamide as a cross-linker. Cross-linker to monomer ratio was set at 1:100, which is the average number of cross-links per number of monomer units in linear subchains. Ammonium persulfate in 3 mM concentration was used as an initiator. All reagents were purchased from Merck (Schuchardt, Hohenbrunn).

In the synthesis of PAAm ferrogels free-radical polymerization was performed in ferrofluids with different concentration of NPs. The composition of the reaction mixture: monomer, cross-linker, and initiator concentration was the same as for the blank PAAm hydrogel. As the gel samples swelled in the consequent washing cycles after the synthesis, the final concentration of NPs in ferrogels changed with respect to the initial concentration set up in the synthesis. The concentration of NPs in ferrogels was determined by the thermogravimetric analysis (NETZSCH STA 409). It was 0.25 or 0.75% of iron oxide NPs in ferrogel by weight.

Polymerization of gels and ferrogels was performed in different master-forms at 80 °C for two hours. Polyethylene probe tubes (diameter 10 mm) were used to form the gel cylindrical samples needed for mechanical and electrical examinations. Upon the polymerization, the gel samples were removed from the probe tubes and washed in distilled water for 2 weeks with water renewal every two days until constant weight of the gel samples was achieved.

Gel samples for the studies of biocompatibility were made in the shape of thin sheets – ca. 1 mm in thickness. Prior to the heating, the reaction mixture was placed between commercial 25 × 25 (mm^2) polished cover glasses for optical microscopy. The glasses were separated by 0.8 mm Al wire spacers provided the thickness of the resulted gel sheet. The synthesized gel sheets were then washed as indicated above. To produce the gel samples for cell culturing in 24-well and 96-well plates, the gel sheets were cut by a round razor blade to appropriate diameter of 13 and 6.5 mm, respectively. Fig. 5 shows the gel and ferrogels samples used for cell culturing.

Magnetic characterization of ferrogels

The magnetization M(H) curves of gel and ferrogels were measured by vibrating sample magnetometer (Faraday magnetometer of laboratory design) using polycarbonate capsules. The value of the magnetization in a field of 1.8 kOe was denominated as saturation magnetization M_s. Hysteresis loop shape for air-dry NPs, as it was mentioned above, reflected no saturation at room temperature: the magnetization in the field of 60 kOe was close to 55 emu/g. Observed magnetic characteristics of NPs (absence of saturation at room temperature, saturation magnetization value, low coercivity) are consistent with close to superparamagnetic

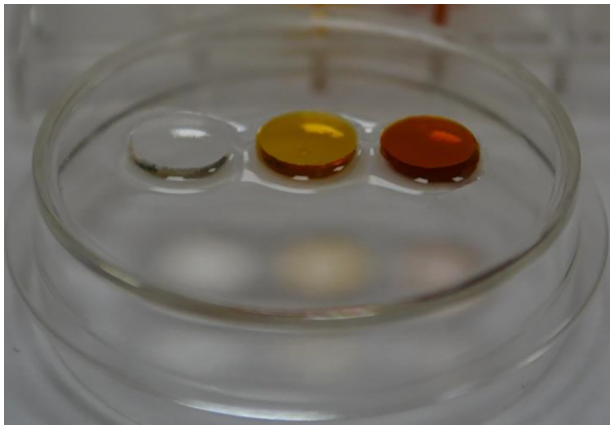

Fig. 5. Examples of gel and ferrogel samples (diameter ~6.5 mm) with the iron oxide NPs content 0, 0.25 or 0.75% (from left to right) used for cell culturing in 96-well plates.

behaviour earlier discussed for the iron oxide NPs obtained in the same conditions [23].

Fig. 6 shows the results of magnetic characterization for gel and selected ferrogel samples with different amount of magnetic filler. As to expect for the water based sample, gel without NPs has linear diamagnetic response. All the ferrogels had S-shaped hysteresis loops with very low the coercivity (H_c) of the order of few Oe, reflecting very weak interactions between the iron oxide NPs. M_s presented a linear dependence on the concentration of NPs. It is important to mention that the shape of M/Ms. hysteresis loops where $M_s = M(H = 1.8$ kOe) was similar for all ferrogels under consideration clearly confirming the similarity of magnetic state of all samples. In all cases under consideration, we are dealing with diluted system in which magnetic interactions are very weak and most probably negligible. The same conclusion comes from the estimation of the average distances between the NPs on the molecular level [22] in the supposition of the de-aggregated state. The average distances between the NPs are at least 10 time larger comparing with average NPs diameter.

Methods

Gel viscoelasticity measurements

Cylindrical gel samples ~10 mm in length and ~10 mm in diameter were used for mechanical testing. The equipment of laboratory design was built around an optical system based on a digital camera, and contained the following parts: a bath for the gel sample, a semiconductor force transducer, an electromagnetic linear motor for applying mechanical deformations, a semiconductor optical transducer for the measurement of gel sample length in dynamics. Gel sample was clamped vertically between the livers of force transducer and linear motor. To produce the 'compression-decompression' cycle of gel samples, the step-wise axial deformations (ε) were applied by means of the linear electromagnetic motor (Fig. 7).

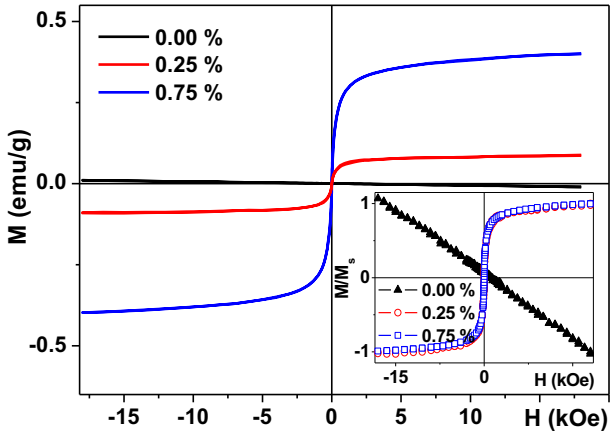

Fig. 6. Hysteresis loops of gel and selected ferrogels with different concentration c of iron oxide NPs. Inset shows the M/Ms. hysteresis loops, where $M_s = M$ (H = 1.8 kOe) calculated for each one of the samples. Numbers are concentrations of NPs of iron oxide in gel (by weight).

Gel tension (σ) was calculated as the recorded force normalized by the gel cross-sectional area. To obtain the correct value of gel cross-section in the course of applied deformations, the diameter of gel sample was monitored at every step by means of digital camera. Young modulus (E) was determined as the slope of linear part of curve in coordinates ε vs σ: $tg\alpha = \sigma/\varepsilon = E$.

The apparent viscosity (η) of gel samples was calculated as: $\eta = E\tau$, where τ is the time constant of force relaxation obtained in the gel after its rectangular deformation of 2.5–5% (see inset for Fig. 7), and calculated using the Maxwell model of viscoelasticity [36].

Gel electrical potential measurements

The electrical potential of gel was obtained by two identical Ag/AgCl tapered glass microelectrodes (~1 μm in tip diameter) typically used in biophysical studies for intracellular voltage measurement. The details of potential measurement in the gel were described in several studies [29,30]. Briefly, thin-walled, single-barrel borosilicate capillary tubes "TW150F-6" ("World Precision Instruments", USA) were single-pulled using a standard electrode puller "ME-3" ("EMIB Ltd", Russia). The pulled electrodes were immersed in a 3 M KCl solution with the tip facing upward, so that the solution climbed to the tip by capillary action.

One electrode was pinned into the gel sample and the other was placed into outside water. The potential difference between microelectrodes was measured using an instrumental amplifier on the base of an integrated circuit "INA 129" ("Burr-Brown", USA). To reduce the influence of electromagnetic interference on the potential difference measurement, special wire shields were provided around the measuring unit.

Gel biocompatibility testing

Cell adhesion to material surfaces as a basic method for the determining of gel samples biocompatibility was studied in the present study. As it well known, the cell adhesion is one of the initial stages of cells monolayer formation, and it characterizes a direct interaction between cells and matrix [37]. Primary cultures of fibroblasts and primary leucocytes were chosen for the first-check of gels biocompatibility. In general, the culturing of fibroblasts is widely introduced in biomedicine, e.g. for the stimulation of bone or skin tissues reparative regeneration, for the creation of bone or cartilage bioimplants etc. The blood cells, in particular leucocytes, initiate *in vivo* inflammatory and regenerative processes in the wound region. Thus, the interaction of fibroblasts and leucocytes with any artificial material is very important test for its future use in the regenerative and transplantation medicine.

The culture of human dermal fibroblast cells (5th passage) was obtained from a supposedly healthy donor of 40 years old. The culture of human peripheral blood leukocytes was derived from five supposedly healthy donors of 23–28 years old. All donors were informed of the procedures and benefits involved in the study before their written consents were obtained. Ethics Committee of the Ural State Medical University approved the study.

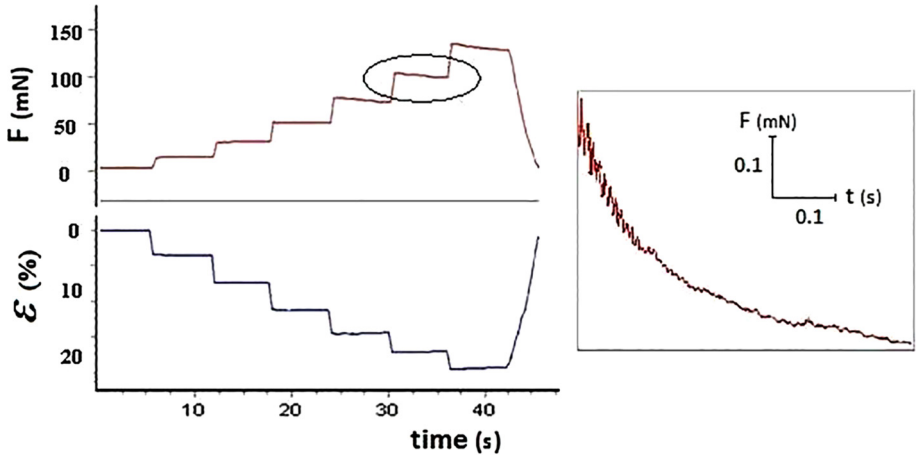

Fig. 7. Experimental records of force measurement in the course of gel sample deformation. Insert (on the right) displays the initial stage of force change in response to the gel compression step.

Determination of the adhesive activity of human dermal fibroblasts to the gels

At the first stage, the gel samples were sterilized in a Dulbecco's Phosphate Buffered Saline (DPBS) purchased from Sigma Aldrich, USA without Ca^{2+} and Mg^{2+} for 30 min at 121 °C, 1.1 atm. The primary culture of dermal fibroblasts was performed by enzymatic disaggregation of skin using collagenase, extracted from Clostridium histolyticum (Sigma Aldrich, USA) [38]. Flap of skin ($\sim$10 mm^2) was removed from the gluteal region of patient.

The cells were spread onto the surface of the gel samples sized for 96-well polystyrene plate (Orange Scientific, Belgium). The sowing concentration of cells was set to 4×10^3 cells per well. The culture medium of Dulbecco's Modified Eagle's Medium – high glucose – DMEM/Ham F-12 – purchased from Sigma Aldrich, USA with 10% fetal bovine serum (Sigma Aldrich, USA) was used. After passage, the cell cultures were incubated at 37 °C, 5% CO_2 and 95% humidity in a Sanyo 18AIC incubator (Japan) for 6 h, and then washed off from unattached cells in DPBS solution without Ca^{2+} and Mg^{2+}.

The fibroblasts adhered to the gel samples were documented with the use of ZOE microscope (Bio-Rad, USA), and then removed from the gel surfaces by the means of 0.25% tripsin-versene solution. The number of attached cells was counted using an automated cell counter Scepter (Millipore, USA). The adhesion index was calculated as the number of adhered cells divided by the number of cells sown and multiplied by 100%.

Eight wells of 96-well polystyrene plate were set for the blank gel and ferrogels with MNPs concentration of 0.25 or 0.75% for each and used for the cells adhesion testing. Additionally, eight free wells were filled with the same sowing concentration of cells to serve as a reference point.

Determination of the adhesive activity of human peripheral blood leucocytes to the gels

The gel samples were immersed in Hank's solution (NPO PanEko, Russia) without phenolic red (pH = 6.8) for one day, and sterilized at 120 °C for 20 min. Subsequently, the gel samples were placed on the bottom of 24-well polystyrene plates (SPL Lifesciences, Castor).

To get leukocytes, the peripheral blood was taken from supposedly healthy donors on an empty stomach at early morning from *v. Intermedia cubiti*, and stored in test tubes (Vacuette TUBE, Greiner Bio-Ont GmbH) containing Lithium Heparin. After sedimentation of erythrocytes, plasma rich in leukocytes was prepared. Ungraded peripheral blood leukocytes were selected and washed in Medium-199 with Earle salts and glutamine (FGU SRC Vector, Russia). The number of cells was counted with the use of Goryaev's chamber, and set to 6×10^6 cells per square centimeter in Medium-199 contained 20% fetal bovine serum (Biosera, Brazil).

The suspension of leukocytes was spread onto the surface the surface of gel samples, and incubated for 2 h at 37 °C, 5% CO_2 and absolute humidity. Then, unattached cells were removed from the samples by gentle washing with 0.9% NaCl solution. Cell morphology and their adhesiveness were assessed with the use of microscope (Micros MC-200, Austria) after cells staining by Romanovsky-Giemsa. The average number of adhered cells in 10 visual fields for every gel sample was calculated [39].

Cells adhesion to the blank gel and ferrogels with MNPs concentration of 0.25 or 0.75% by weight was tested in six samples of each gel. In total, 90 samples for five donors were studied.

Statistical analysis

The statistic software packages "SPSS Statistics 17.0" (IBM) and "RStudio" (Version 0.99.903, RStudio, Inc.) were used for statistical analysis. Mann-Whitney test and t-test were applied for comparative analysis of biological and physical data sets, respectively. The level of significance was set at $p < 0.05$.

Results and discussion

Impact of nanoparticles on the viscoelasticity of gels

Fig. 8 shows an example of the dependence of tension vs deformation obtained for the blank gel and ferrogel filled with iron oxide NPs in concentration 0.75% by weight. One can see that (1) the dependence of gel tension on gel deformation is not linear if the whole deformation interval of 0 to 25% is considered; (2) the addition of iron oxide NPs into the polymer network shifts "tension vs deformation" curve upwards. Young modulus of $\sim$25 kPa for gel and $\sim$40 kPa for ferrogel were calculated based on the linear part of the "tension vs deformation" curves.

Table 1 shows the results of Young modulus and effective viscosity calculations in the blank gel and ferrogels with different concentrations of NPs. One can see that the gradual increase of MNPs concentration is accompanied by the significant increase of Young modulus. Apparent viscosity grows up with the addition of 0.25% of NPs to the gel and then remains stable with the further increase of NPs concentration.

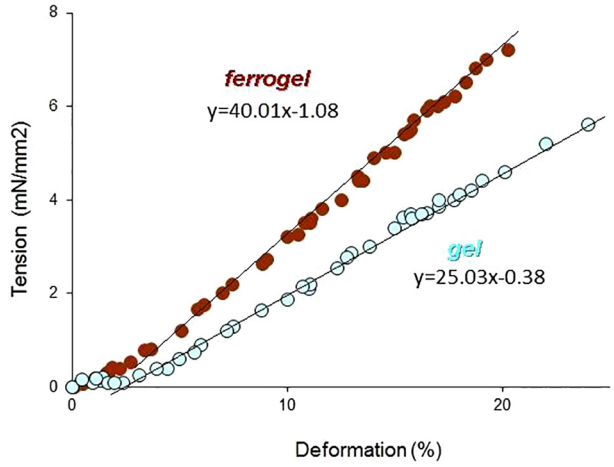

Fig. 8. Effect of MNPs embedded in PAAm gel matrix on the deformation curve of the gel or ferrogel. Blue circles correspond to the gel without NPs, brown ones – to ferrogel with 0.75% NPs by weight. (For interpretation of the references to colour in this figure legend, the reader is referred to the web version of this article.)

Table 1
Mean values and SD of Young modulus and apparent viscosity in tested gel samples (n = 9).

Samples	Young Modulus (E, kPa)	Effective viscosity (η, kPa × s)
Gel	26.50 ± 1.7	5.8 ± 1.2
Ferrogel (NPs – 0.25%)	32.3 ± 1.3 $p < 0.05$	8.4 ± 2.1 $p < 0.01$
Ferrogel (NPs – 0.75%)	39.5 ± 1.5 $p < 0.001$	8.6 ± 1.8 $p < 0.01$

Both the Young modulus and the apparent viscosity increase with the concentration of iron oxide NPs in the ferrogel. Unexpectedly, this increase is much higher than that, predicted by the classical theories of composite materials [40]. The structural reasons underlying this strong effect are unclear. Possibly, during the gel polymerization NPs aggregate to a certain extent and form various structures, whose influence on the mechanical properties of the composite is much stronger than the effect of the individual particles.

It should be noted that non-monotonic dependences of the viscoelastic module on the concentration of embedded rigid NPs (with one maximum shape) were observed in experiments with various gels [41,42]. The physical reason of this effect is still unclear. It can be a result of chemical interaction of the ions, disrobed from the NPs surfaces, with the gel macromolecules. This interaction can inhibit the gel polymerization, reducing its elastic and viscous module [41]. The second reason can be an agglomeration of the NPs and the fragments of the macromolecules into mesoscopic dense aggregates. Because of such kind agglomeration, the concentration of macromolecules in the main part (out of the aggregates) of the gel decreases, provoking the decrease of the mechanic module of composite [43].

Although more studies is necessary in order to understand an apparent viscosity increase we can mention some interesting directions for further research. It is well known that the largest particles out of particle distribution in ferromagnetic suspension play a decisive role in the agglomeration process [44]. The idea to include magnetic interactions for the description of the behaviour of ferrogels with multidomain nanoparticles is under special focus of the present day research [45]. In the same way as large NPs contribute to colloidal agglomeration they may keep NPs agglomerates stable in the course of mechanical deformation. It would be interesting to test ferrogels containing magnetic nanoparticles with different parameters of particle size distribution and even on purpose created ensembles with bimodal distributions (having a small fraction of large multidomain iron oxide NPs).

One of the direction to answer the question about the role of magnetic interactions for the description of the behaviour of ferrogels with large nanoparticles would be a systematic comparison of viscoelastic properties of gels filled with nanoparticles assembles having similar size distribution characteristic but being either magnetic or non-magnetic. This research direction is strictly dependent on the improvements of nanoparticle fabrication methods. One of the promising techniques with this respect is the electric explosion of wire [46].

In general, the obtained results show that at a given levels of the PAAm network density (1:100) and the iron oxide NPs concentration (0.25 or 0.75 wt%), the ferrogels elasticity is suitable for polymeric scaffolds used in the muscle tissue engineering [12,47].

Impact of nanoparticles on the electrical potential of gels

Fig. 9 shows the typical experimental plot of the electrical potential (φ) measurement in the ferrogel sample by a capillary microelectrode. The baseline with $\varphi = 0$ corresponds to the case of allocation of an electrode in a supernatant solution outside the gel sample. Upon pinning the capillary electrode into the gel, its potential dropped down to the value ca. −60 mV, which remained constant. When the electrode was taken out, the electrical potential returned to the baseline. Table 2 presents the values of the electrical potential in all tested gel samples. One can see that in the ferrogels the negative values of electrical potential are significantly higher than that in the blank gel.

The difference of the electrical potentials between the gel and its surroundings is a consequence of Donnan equilibrium in a two-phase system with the restricted diffusion of one of the ions across the phase boundary [48]. In polyelectrolyte gel it stems from the general asymmetry of charge distribution in the electrically charged polymeric network. On the one hand, the gel macromolecular network comprises electrical charges, which are affixed by the polymeric chains without possibility to leave the gel. On the other hand, these charges are equilibrated by the equivalent amount of oppositely charged counterions, which are free to move both inside and outside the network and establish an equilibrium distribution. Such equilibrium (Donnan equilibrium) results in the existence of the electric potential, which has the same sign as the sign of the electrical charges affixed upon the subchains. The sign is negative for the polyanionic gels and positive for the polycationic gels [29,34,49,50].

In the present work, we used PAAm gel. Acrylamide is a neutral monomer and PAAm gel is not a polyelectrolyte, which means that

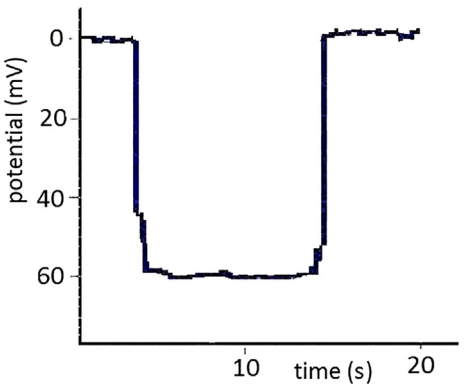

Fig. 9. Typical experimental record of the electrical potential obtained in the ferrogel with iron oxide NPs concentration of 0.75%.

Table 2
Mean values and SD of electrical potential in tested gel samples (n = 10).

Samples	Potential, mV
Gel	−22.5 ± 3.6
Ferrogel (NPs – 0.25%)	−68.8 ± 9.4 $p < 0.001$
Ferrogel (NPs – 0.75%)	−62.3 ± 5.3 $p < 0.001$

the network does not contain electrical charges on the subchains and counterions. Nevertheless, we observed negative electrical potential −23 ± 4 mV for the blank gel. The possible reason for the non-zero potential might be rationalized by considering the details of microelectrode technique elaborated for the measurements of potential. In fact, in this technique the basic quantity is the diffusion potential of KCl solution across the tip of the microelectrode, which is pinned into the gel [50]. Thus, the microelectrode technique measures the difference in the diffusion potentials of KCl in water (outside the gel) and in the gel. It is possible that the diffusion potential of KCl in the gel changes due to the presence of hydrocarbon subchains of the network, affecting the dielectric constant of the gel as compared to that of water. It might shift the measured potential of the gel to the negative value. In this respect the potential of the blank PAAm hydrogel should not be considered as Donnan potential.

Meanwhile, the substantial increase of the potential for the ferrogels certainly stems from the Donnan equilibrium, which is established if NPs are embedded into the polymeric network. As it was indicated in the experimental section, the iron oxide NPs in ferrofluid were electrostatically stabilized by sodium citrate to prevent their aggregation. Citrate anions readily absorb on the surface of NPs and provide the negative electrical charge of the particles. Na^+ cations are counterions in the double electrical layer on the surface of iron oxide NPs. During the synthesis of ferrogels the polymeric network encapsulates the NPs with the double electrical layers on their surface. Thus, the negatively charged particles became entrapped in the network and can not leave it. Na^+ counterions remained free to move and to establish equilibrium distribution between gel and outside water. It is the basis for the negative Donnan potential of the ferrogel to appear. It is remarkable, although might be coincidental as well, that the potential of the ferrogels (63–69 mV) is close to the simple sum of the baseline potential of the blank PAAm gel (23 mV) and the zeta-potential of ferrofluid (−30 mV).

Impact of nanoparticles on the adhesive activity of cells

Fig. 10 shows photographs of the human dermal fibroblasts attached to the blank gel and to the ferrogels with iron oxide NPs concentrations of 0.25 or 0.75%. Visually, the number of cells depends on the NPs concentration embedded in the gel matrix. Furthermore, the overwhelming majority of cells adhered to the blank gel mainly resembles a sphere in shape while the cell spreading take place in the ferrogels. In the ferrogel, the number of spindle-shaped fibroblasts grows with the increase of NPs concentration. This morphological observation implies a good affinity of the fibroblasts to ferrogels.

Fig. 11 shows the effect of iron oxide NPs concentration in PAAm gel on the adhesion activity of human dermal fibroblasts. One can see that the increase of NPs concentration in the gel network results in the increase of the cell adhesion index. At NPs concentration of 0.75%, the cell adhesion to the ferrogel is significantly higher than that for the blank gel ($n = 8$, $p < 0.01$). It is also seen that the more the NPs concentration the closer is the adhesion index to the polystyrene (control) widely introduced for the cellular technologies.

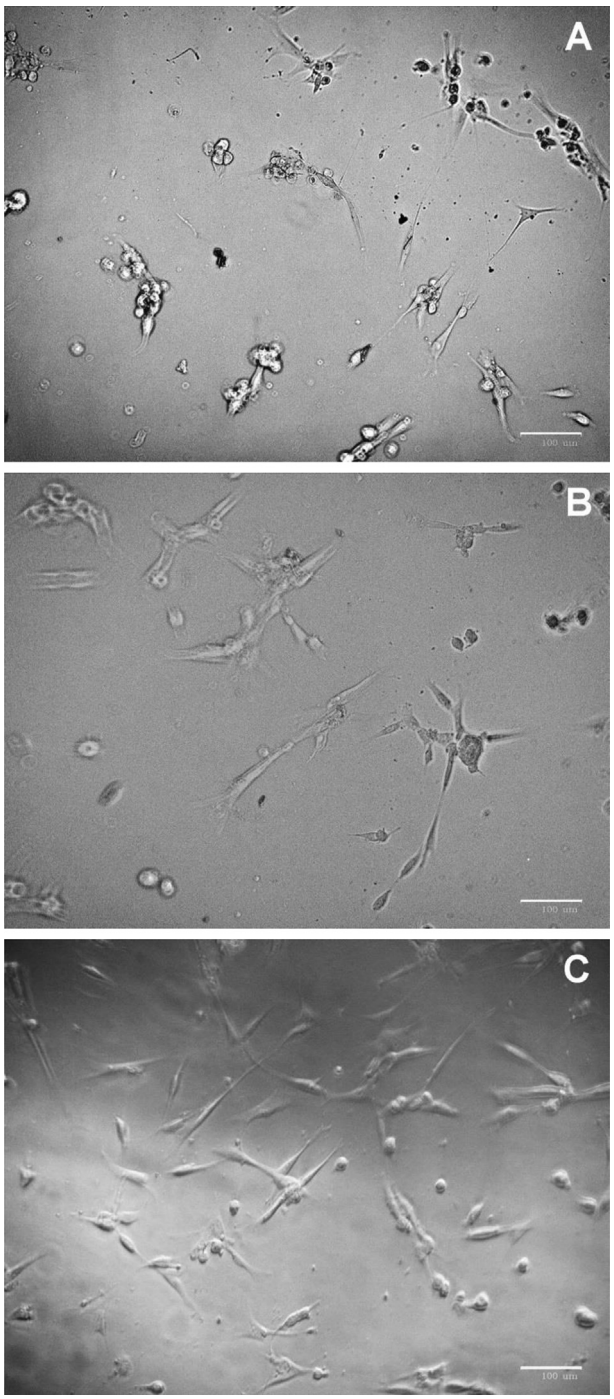

Fig. 10. A gallery of photos obtained for human dermal fibroblasts in PAA gels with different concentration of iron oxide NPs (see explanation in the text). A – blank gel, B – ferrogel with 0.25% of iron oxide NPs, C – ferrogel with 0.75% of NPs. Scale bars are equal to 100 μm.

Table 3 presents the results of human peripheral blood leucocytes adhesiveness to the blank gel and ferrogels with iron oxide NPs concentration of 0.25 or 0.75%. In that case, to estimate the impact of NPs on the cell adhesion quantitatively the number of cells attached to the ferrogels was normalized to the number of cells adhered to the blank gel. One can see that in the blank gels the adhesion approximately in 1.5 and 1.8 times lower than that one in the ferrogels with NPs concentration of 0.25% or 0.75%, accordingly.

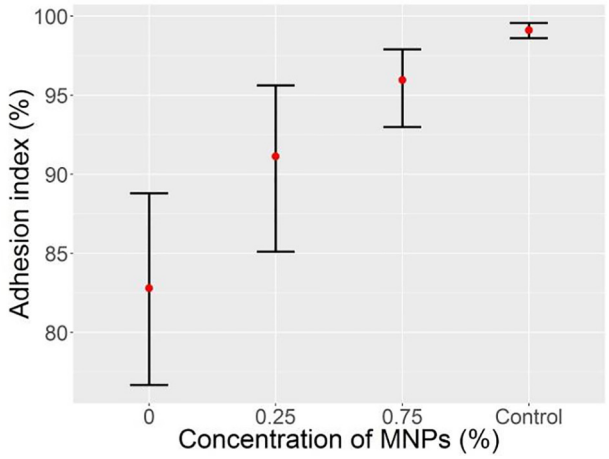

Fig. 11. Results of adhesion index calculation for the human dermal fibroblasts in different gel samples and the control matrix. The adhesion index was defined as the number of adhered cells divided by the number of cells sown and multiplied by 100%. Mean values (n = 8) and confidence interval (p = 0.05) as vertical bars are plotted.

Table 3
Adhesive activity of the human peripheral blood leucocytes to PAAm gels with different concentration of iron oxide NPs. Mean values (n = 30) and confidence interval (p = 0.05) are present.

Samples	Relative Adhesion, %
Gel	100 ± 5
Ferrogel (NPs – 0.25%)	153 ± 15
Ferrogel (NPs – 0.75%)	181 ± 13

Thus, the adhesive activity of the human peripheral blood leucocytes and the human dermal fibroblast showed qualitatively the same results. In general, the direct and indirect effects of iron oxide NPs on the cell adhesion are possible. Although known data on the direct impact of iron oxide nanoparticles on the cell function are quite contradictory, the authors of a number of studies have noted the increase of cell adhesion to substrates in the presence of iron oxide NPs [23,51–54]. The indirect effect of NPs on the cell adhesion due to the increase of gel stiffness [55–58], to the change of gel electrical potential [59,60], and to possible change of gel surface smoothness and 3D structure [47] are most likely arguments to explain the obtained findings.

Topography alterations of the gels and also the clustering effect are very important determinants of the different cell behaviour. With respect to formation of clusters, aggregation is almost inevitable process related to ferrofluid system. The second reason can be an agglomeration of the NPs and the fragments of the macromolecules into mesoscopic dense aggregates during polymerization process. Here we would like to come back and remind that the major fraction of particles in ferrofluid corresponds to the individual NPs (80 wt%) whereas the minor fraction of small aggregates is still present (20 wt%). This means that aggregates of NPs can be incorporated into the gel matrix as mesoscopic dense aggregates providing the statistical random distribution of inhomogeneities.

In addition, one can also imagine more exotic factors responsible for enhanced cell adhesion in the case of ferrogels with high NPs concentrations. Such environmental factors as terrestrial magnetic field, electromagnetic radiation always appearing in non-shielded room and microvibrations might be involved and contributing. For separation each one of these factors "clean" environments should be created for systematic experiments.

Meanwhile, independently on the mentioned factors or their combination affecting the result, the increase of iron oxide NPs concentration in ferrogel improves PAAm gel biocompatibility estimated by the cell adhesion activity. Adhesion phenomenon did not depend on the type of cells. Qualitatively, the findings presented here are in a good agreement with the results obtained by other researchers for polyvinyl alcohol (PVA) hydrogels filled with Fe_2O_3 NPs [25,26]. The authors showed that the osteoblasts preferentially adhered to ferrogels, and with the increasing NPs concentration, the cell adhesion density was significantly promoted.

Thus, the screening assessment of cells morphology and adhesion activity showed promising use of PAAm ferrogels for the tissue engineering purposes. However, future investigations of the cells proliferation and differentiation in PAAm ferrogels with different topography and NPs distribution are necessary, especially in a condition of the external magnetic field application.

Conclusions

This study addresses the development of gel-based magnetic material for possible use in the biomedical applications in the fields of tissue engineering, regenerative medicine, drugs delivery and magnetic biosensing. Polyacrylamide gel was chosen as a soft working body because of its biocompatibility is well known. The gel was filled with the maghemite γ-$Fe_{2.04}O_{2.96}$ NPs also well introduced in the biomedicine. Ferrogels were synthesized by radical polymerization of acrylamide in a stable aqueous suspension of NPs (d_w = 18.5 nm) fabricated by laser target evaporation. The gel network density was set to 1:100, the concentration of imbedded NPs was fixed at 0, 0.25 or 0.75% by weight.

The main task of proposed investigation was to determine the effects of iron oxide NPs on the physical properties of gel and its biocompatibility. We started from the gel viscoelasticity and potential testing because the both the mechanical and the electrical features of gel are critical for the tissue engendering. The inclusion of iron acid NPs into the polymer network with concentration of 0.25 or 0.75% by weight resulted in the significant increase of Young modulus and electrical potential in the gel. Moreover, the more the NPs concentration the more were stiffness and potential of gels. At the same time, the embedding of NPs to the gel network shifts negative value of gel potential toward the living cells potential.

The impact of iron oxide NPs on the gel physical properties is a reasonable basis to explain our finding on the increase of cell adhesion to ferrogels. The cell adhesiveness is an important measure of cells interaction with matrix, and it reflects the biocompatibility of material directly. We found that the biocompatibility is significantly higher in ferrogels than that in the blank gel. Importantly, this conclusion is true for the both the human dermal fibroblasts and the human peripheral blood leucocytes. Since these cells belong to different physiological systems, the obtained results imply the wide-range of ferrogel promising use for specific needs of biomedicine. This may be the magnetically controlled multilayer wound healing coatings, bioimplants of musculoskeletal tissue, micro-devices for drugs targeted delivery and controlled release, magnetic biosensors. However, future investigations of the cells proliferation and differentiation in PAAm ferrogels as well as detailed studies of the effect of the ferrogel matrix on the cell structure and functioning are necessary.

Thus, from the viewpoint of biomedical engineering applications, the inclusion of small amount of iron oxide NPs into the polymer network of PAAm gel significantly enhances the

mechanical and electrical properties of ferrogels, and improves biocompatibility of these systems. Meanwhile, the question to what extent the magnetism of NPs is responsible for the observed behaviour at the moment remains open.

Conflict of interest

The authors have no conflict of interest to declare.

Acknowledgements and funding

The assistance of Dr. A.I. Medvedev and Dr. A.M. Murzakaev in XRD and TEM characterization of iron oxide NPs is highly appreciated. We thank A.D. Baldanshirieva, A.V. Korotkov, D.A. Sichkar, M.A. Rusinova and Dr. S.Yu. Sokolov for special support. In part, the Russian Foundation for Basic Research (## 16-08-00609-a, 16-58-12003) and the Program of Russian Federation Ministry of Science and Education (# 3.1438.2017/PCh) supported this work. Selected measurements were done at SGIKER services of UPV-EHU.

References

[1] Jun Y-W, Seo J-W, Cheon J. Nanoscaling laws of magnetic nanoparticles and their applicabilities in biomedical sciences. Acc Chem Res 2008;41:179–89.
[2] Owens D, Peppas N. Opsonization, biodistribution, and pharmacokinetics of polymeric nanoparticles. Int J Pharm 2006;307:93–102.
[3] Baselt D, Lee G, Natesan M, Metzger S, Sheehan P, Colton R. A biosensor based on magnetoresistance technology. Biosens Bioelectron 1998;13:731–9.
[4] Liu T, Hu S, Liu T, Liu D, Chen S. Magnetic-sensitive behaviour of intelligent ferrogels for controlled release of drug. Langmuir 2006;22:5974–8.
[5] Harland R, Prudhomme R. Polyelectrolyte gels: properties, preparation and applications. Washington DC: American Chemical Society; 1992.
[6] Philippova OE. Responsive polymer gels. Polym Sci Ser C 2000;42(2):208–28.
[7] Hirotsu S. Responsive gels: volume transitions II, Advances in polymer sciences. Berlin: Springer-Verlag; 1993.
[8] Ling GN. A revolution in the physiology of the living cell. Malabar, Fl: Krieger Pub. Co.; 1992.
[9] Pollack G. Cells, gels and the engines of life. Seattle WA: Ebner & Sons; 2001.
[10] Shahinpoor M, Kim KJ, Mojarrad M. Artificial muscles: applications of advanced polymeric nanocomposites. New York, London: CRC Press, Taylor & Francis Group; 2007.
[11] Shklyar TF, Safronov AP, Toropova OA, Pollack GH, Blyakhman FA. Mechanoelectric potentials in synthetic hydrogels: Possible relation to cytoskeleton. Biophysics 2010;55:931–6.
[12] DeRossi D, Kajiwara K, Osada Y, Yamauchi A. Polymer gels: fundamentals and biomedical applications. New York: Plenum; 1991.
[13] Shahinpoor M, Kim K. Ionic polymer–metal composites: III. Modeling and simulation as biomimetic sensors, actuators, transducers, and artificial muscles. Smart Mater Struct 2004;13:1362–88.
[14] Pelham R, Wang Y-L. Cell locomotion and focal adhesions are regulated by substrate flexibility. Proc Natl Acad Sci USA 1997;94:13661–5.
[15] Kandow C, Georges P, Janmey P, Beningo K. Polyacrylamide hydrogels for cell mechanics: steps toward optimization and alternative uses. Methods Cell Biol 2007;83:29–46.
[16] Rentong Y, Zheng S. Poly(acrylic acid)-grafted Poly(N-isopropyl acrylamide) networks: preparation, characterization and hydrogel behaviour. J Biomater Sci 2011;22:2305–24.
[17] Vignaud T, Ennomani H, Théry M. Polyacrylamide hydrogel micropatterning. Methods Cell Biol 2014;120:93–116.
[18] Qin J, Asempah I, Laurent S, Fornara A, Muller R, Muhammed M. Injectable superparamagnetic ferrogels for controlled release of hydrophobic drugs. Adv Mater 2009;21:1354–7.
[19] van Bruggen M, van Zon J. Theoretical description of a responsive magneto-hydrogel transduction principle. Sens Actuators, A 2010;158:240–8.
[20] van Berkum S, Dee J, Philipse P, Erne B. Frequency-dependent magnetic susceptibility of magnetite and cobalt ferrite nanoparticles embedded in PAA hydrogel. Int J Mol Sci 2013;14:10162–77.
[21] Pankhurst Q, Connolly J, Jones S, Dobson J. Applications of magnetic nanoparticles in biomedicine. J Phys D: Appl Phys 2003;36:R167–81.
[22] Kurlyandskaya GV, Fernandez E, Safronov AP, Svalov AV, Beketov IV, Burgoa Beitia A, et al. Giant magnetoimpedance biosensor for ferrogels detection: model system to evaluate properties of natural tissue. Appl Phys Lett 2015;106:193702.
[23] Kurlyandskaya GV, Novoselova IuP, Schupletsova VV, Andrade R, Dunec NA, Litvinova LS, et al. Nanoparticles for magnetic biosensing systems. J Magn Magn Mater 2017;431:249–54.
[24] Li Y, Huang G, Zhang X, Li B, Chen Y, Lu T, et al. Magnetic hydrogels and their potential biomedical applications. Adv Func Matters 2013;3:660–72.
[25] Hou R, Zhang G, Du G, Zhan D, Cong Y, Cheng Y, et al. Magnetic nanohydroxyapatite/PVA composite hydrogels for promoted osteoblast adhesion and proliferation. Colloids Surf, B 2013;103:318–25.
[26] Hou R, Nie L, Du G, Xiong X, Fu J. Natural polysaccharides promote chondrocyte adhesion and proliferation on magnetic nanoparticle/PVA composite hydrogels. Colloids Surf, B 2015;132:146–54.
[27] Safronov AP, Shakhnovich MA, Kalganov A, Shklyar TF, Blyakhman FA, Pollack GH. Periodic bending of polyelectrolyte gels in dc electric field. Polymer 2011;52:2430–6.
[28] Blyakhman FA, Safronov AP, Shklyar TF, Filipovich MA. To the mechanism of polyelectrolyte gel periodic acting in the constant DC electric field. Sens Actuators, A 2015;229:104–9.
[29] Shklyar T, Dinislamova O, Safronov A, Blyakhman F. Effect of cytoskeletal elastic properties on the mechanoelectrical transduction in excitable cells. J Biomech 2012;45:1444–9.
[30] Blyakhman FA, Safronov AP, Zubarev AYu, Shklyar TF, Dinislamova OA, Lopez-Lopez MT. Mechanoelectrical transduction in the hydrogel-based biomimetic sensors. Sens Actuators, A 2016;248:54–61.
[31] Osipov VV, Platonov VV, Uimin MA, Podkin AV. Laser synthesis of magnetic iron oxide nanopowders. Tech Phys 2012;57:543–9.
[32] Safronov AP, Beketov IV, Komogortsev SV, Kurlyandskaya GV, Medvedev AI, Leiman DV, et al. Spherical magnetic nanoparticles fabricated by laser target evaporation. AIP Adv. 2013;3:052135.
[33] Safronov AP, Beketov IV, Tyukova IS, Medvedev AI, Samatov OM, Murzakaev AM. Magnetic nanoparticles for biophysical applications synthesized by high-power physical dispersion. J Magn Magn Mater 2015;383:281–7.
[34] Safronov AP, Kamalov IA, Shklyar TF, Dinislamova OA, Blyakhman FA. Activity of counterions in hydrogels based on poly(acrylic acid) and poly(methacrylic acid): Potentiometric measurements. Polym Sci, Ser A 2012;54:909–19.
[35] Coey JMD. Magnetism and magnetic materials. New York: Cambridge University Press; 2010.
[36] Bartenev G, Frenkel S. Physics of polymers. Leningrad: Khimiya; 1990.
[37] Barry M. Cell Adhesion: the molecular basis of tissue architecture and morphogenesis. Cell 1996;84:345–57.
[38] Makeev OG, Zubanov PS, Ulybin A. RU Pat., 2345781; 2009.
[39] Moiseeva O, Villevalde S, Emelyanov I, Ivanova T. Comparative research of enalapril and atenolol antihypertensive efficacy in high risk patients. Ration Pharmacoth Cardiol 2006;2:19–25.
[40] Cristensen R. Mechanics of composite materials. New York: Wiley; 1979.
[41] Günther D, Borin DYu, Günther S, Odenbach S. X-ray micro-tomographic characterization of field-structured magnetorheological elastomers. Smart Mater Struct 2012;21:015005.
[42] Albani D, Gloria A, Giordano C, Rodilossi S, Russo T, D'Amora U, et al. Hydrogel-based nanocomposites and mesenchymal stem cells: a promising synergistic strategy for neurodegenerative disorders therapy. The Sci World J 2013;2013:270260. https://doi.org/10.1155/2013/270260.
[43] Bonhome-Espinosa AB, Campos F, Rodriguez IA, Carriel V, Marins JA, Zubarev A, et al. Effect of particle concentration on the microstructural and macromechanical properties of biocompatible magnetic hydrogels. Soft Matter 2017;13:2928.
[44] Hubert A, Schäfer R. Magnetic domains: the analysis of magnetic microstructures. Berlin Heidelberg: Springer-Verlag; 2008.
[45] Shankar A, Safronov A, Mikhnevich E, Beketova I, Kurlyandskaya G. Ferrogels based on entrapped metallic iron nanoparticles in a polyacrylamide network: extended Derjaguin–Landau–Verwey–Overbeek consideration, interfacial interactions and magnetodeformation. Soft Matter 2017. https://doi.org/10.1039/c7sm00534b.
[46] Kotov YuA. Electric explosion of wires as a method for preparation of nanopowders. J Nanopart Res 2003;5:539–50.
[47] Trappmann A, Gautrot J, Connelly J, Strange D, Li Y, Oyen M, et al. Extracellular-matrix tethering regulates stem-cell fate. Nat Mater 2012;11:642–9.
[48] IUPAC Compendium of Chemical Terminology; 1997.
[49] Gao F, Reitz FB, Pollack GH. Potentials in anionic polyelectrolyte hydrogels. J Appl Polym Sci 2003;89:1319–21.
[50] Guo H, Kurokawa T, Takahata M, Hong W, Katsuyama Y, Uo F, et al. Quantitative observation of electric potential distribution of brittle polyelectrolyte hydrogels using microelectrode technique. Macromolecules 2016;49:3100–8.
[51] Pareta R, Taylor E, Webster T. Increased osteoblast density in the presence of novel calcium phosphate coated magnetic nanoparticles. Nanotechnology 2008;19:265101.
[52] Yang J-X, Tang W-L, Wang X-X. Superparamagnetic iron oxide nanoparticles may affect endothelial progenitor cell migration ability and adhesion capacity. Cytotherapy 2010;12:251–9.
[53] Sun J, Wang S, Zhao D, Hun FH, Weng L, Liu H. Cytotoxicity, permeability, and inflammation of metal oxide nanoparticles in human cardiac microvascular endothelial cells. Cell Biol Toxicol 2011;27:333–42.
[54] Yun H, Lee E, Kim M, Kim J, Lee J, Lee H, et al. Magnetic nanocomposite scaffold-Induced stimulation of migration and odontogenesis of human dental pulp cells through integrin signaling pathways. PLoS One 2015. https://doi.org/10.1371/journal.pone.0138614e0138614.
[55] Discher A, Janmey P, Wang Y. Tissue cells feel and respond to the stiffness of their substrate. Science 2005;310:1139–43.

[56] Engler A, Sen S, Sweeney H, Discher D. Matrix elasticity directs stem cell lineage specification. Cell 2006;126:677–89.
[57] Cretu A, Castagnino P, Assoian R. Studying the effects of matrix stiffness on cellular function using acrylamide-based hydrogels. J Visualized Exp 2010;10: e2089. https://doi.org/10.3791/2089.
[58] Mullen A, Vaughan T, Billia K, McNamara L. The effect of substrate stiffness, thickness, and cross-linking density on osteogenic cell behavior. Biophys J 2015;108:1604–12.
[59] Chen Y, Shiraishia N, Satokawa H, Kakugoa A, Naritaa T, Gong J, et al. Cultivation of endothelial cells on adhesive protein-free synthetic polymer gels. Biomaterials 2005;26:4588–96.
[60] Singh K, Patel K, Lee J, Lee E, Kim J-H, Kim T-H, et al. Potential of magnetic nanofiber scaffolds with mechanical and biological properties applicable for bone regeneration. PLoS One 2014. https://doi.org/10.1371/journal.pone.0091584.